Received: 31 May 2019 | Revised: 9 December 2019 | Accepted: 9 December 2019

DOI: 10.1096/fj.201901361RR

RESEARCH ARTICLE

THE FASEB JOURNAL

Optogenetic-induced sympathetic neuromodulation of brown adipose tissue thermogenesis

Carey E. Lyons[1,2] | Maria Razzoli[1] | Erin Larson[3] | Daniel Svedberg[1] | Andrea Frontini[4] | Saverio Cinti[5] | Lucy Vulchanova[3] | Mark Sanders[6] | Mark Thomas[3] | Alessandro Bartolomucci[1]

[1]Department of Integrative Biology and Physiology, University of Minnesota, Minneapolis, Minnesota

[2]Graduate Program in Neuroscience, University of Minnesota, Minneapolis, Minnesota

[3]Department of Neuroscience, University of Minnesota, Minneapolis, Minnesota

[4]Department of Public Health, Experimental and Forensic Medicine, University of Pavia, Pavia, Italy

[5]Department of Experimental and Clinical Medicine, Università Politecnica delle Marche, Ancona, Italy

[6]University Imaging Center, University of Minnesota, Minneapolis, Minnesota

Correspondence
Alessandro Bartolomucci, Department of Integrative Biology and Physiology, University of Minnesota, Minneapolis, MN 55455.
Email: abartolo@umn.edu

Funding information
Wallin Neuroscience Discovery Fund, Grant/Award Number: NA; HHS | NIH | National Institute of Diabetes and Digestive and Kidney Diseases (NIDDK), Grant/Award Number: DK117504; HHS | NIH | National Institute of Diabetes and Digestive and Kidney Diseases (NIDDK), Grant/Award Number: DK102496; HHS | NIH | National Institute of Diabetes and Digestive and Kidney Diseases (NIDDK), Grant/Award Number: DK118150; HHS | NIH | National Institute of Diabetes and Digestive and Kidney Diseases (NIDDK), Grant/Award Number: DK102496-02S1; UNIVPM, Grant/Award Number: RSA-Frontini; Core

Abstract

The brown adipose tissue (BAT) is a thermogenic organ that plays a major role in energy balance, obesity, and diabetes due to the potent glucose and lipid clearance that fuels its thermogenesis, which is largely mediated via sympathetic nervous system activation. However, thus far there has been little experimental validation of the hypothesis that selective neuromodulation of the sympathetic nerves innervating the BAT is sufficient to elicit thermogenesis in mice. We generated mice expressing blue light-activated channelrhodopsin-2 (ChR2) in the sympathetic nerves innervating the BAT using two different strategies: injecting the BAT of C57Bl/6J mice with AAV6-hSyn-ChR2 (H134R)-EYFP; crossbreeding tyrosine hydroxylase-Cre mice with floxed-stop ChR2-EYFP mice. The nerves in the BAT expressing ChR2 were selectively stimulated with a blue LED light positioned underneath the fat pad of anesthetized mice, while the BAT and core temperatures were simultaneously recorded. Using immunohistochemistry we confirmed the selective expression of EYFP in TH positive nerves fibers. In addition, local optogenetic stimulation of the sympathetic nerves induced significant increase in the BAT temperature followed by an increase in core temperature in mice expressing ChR2, but not in the respective controls. The BAT activation was also paralleled by increased levels of pre-UCP1 transcript. Our results demonstrate that local optogenetic stimulation of the sympathetic nerves is sufficient to elicit BAT and core thermogenesis, thus suggesting that peripheral neuromodulation has the potential to be exploited as an alternative to pharmacotherapies to elicit organ activation and thus ameliorate type 2 diabetes and/or obesity.

Abbreviations: ChR2, channelrhodopsin-2; EYFP, enhanced yellow fluorescent protein; UCP1, uncoupling protein 1.

Carey E. Lyons and Maria Razzoli are co-first authors.

KEYWORDS
AAV6, CLARITY, opsin, peripheral nervous system, UCP1

1 | INTRODUCTION

The brown adipose tissue (BAT) is a thermogenic organ that plays a major role in energy balance through potent glucose and lipid clearance required to fuel its thermogenesis,[1-3] and has been demonstrated to be present and functional in adult humans.[4-8] BAT activation is regulated by central nervous system neural networks which respond reflexively to the thermal afferent signals from skin thermoreceptors.[9] These networks mount an activation of the sympathetic nerves that innervate the BAT, classically in response to either cold acclimation, acute cold exposure[1,2] or stress.[10-12] Brown adipocyte activity is primarily regulated by the sympathetic nerve-derived norepinephrine (NE) signaling through β-adrenergic receptors (βARs) which results in activation of uncoupling protein 1 (UCP1) and consequent conversion of energy to heat.[1,9,13,14] Denervation leads to a dysfunctional BAT composed of UCP1-depleted adipocytes, low thermogenesis, cold intolerance, and vulnerability to obesity,[1,9,15,16] while electrical nerve stimulation elicits a thermogenic effect.[9,10] Adult humans reportedly experience only a modest basal activation of the BAT due to multiple factors, including higher body weight:surface area ratio, predominant exposure to thermoneutral comfort zone, low sympathetic tone to fat pads, and low NE/βAR signaling compared to rodents.[17,18] In humans, BAT activity or amount is inversely associated with obesity and functional measures of diabetes,[4,17] thus suggesting that targeting BAT activation could be a viable therapeutic approach to address obesity.[5,12,19,20] Based on the large body of evidence demonstrating a necessary and sufficient role for sympathetic nerves to regulate BAT differentiation and function,[1,9] and recent studies suggesting that optogenetic stimulation of brown and white adipose tissue can regulate organ function,[21,22] we used two independent approaches in which the expression of the blue light-activated ChR2 is restricted to the sympathetic neurons by either crossbreeding tyrosine hydroxylase (TH)-Cre mice with Rosa26-LSL-ChR2-EYFP,[22] or by intra BAT injection of a retrograde AAV6-hSyn-ChR2-EYFP virus.

2 | MATERIAL AND METHODS

2.1 | Animals and experimental models

C57BL/6J male mice were purchased from Jackson Laboratories at 4-5 weeks of age. We generated TH-Cre X Rosa26-LSL-ChR2-EYFP mice as previously established[22] (referred to as $ChR2^{TH\text{-}Cre+}$ or $ChR2^{TH\text{-}Cre-}$). Founder mice of either strain (TH-Cre B6.Cg-Tg (Th-cre)1Tmd/J, JAX #008601 and Rosa26-LSL-ChR2-EYFP B6.Cg-Gt (ROSA)26Sor/J, JAX #024109) were purchased from Jackson labs in 2017. Our breeding scheme aimed at establishing the Rosa-LSL-ChR2-EYFP locus in homozygosity. Mice derived from this breeding were used in the next ~12 months in the experiments described below. Both male and female TH-Cre X Rosa26-LSL-ChR2-EYFP mice were used and, after confirming that sex did not affect the physiological effect, data from male and females were combined for each experimental treatment. Mice were housed at room temperature with 12-h light:dark cycle. All experimental procedures were approved by the Institutional Animal Care and Use Committee (IACUC) of the University of Minnesota.

2.2 | Viral injections

C57BL/6J male mice were injected with optogenetic vectors under aseptic conditions. Mice were initially anesthetized with a ketamine/xylazine mixture (100 and 10 mg/kg, ip) and were given supplemental ketamine (~ 33 mg/kg, ip) to maintain them at an appropriate anesthetic depth for the duration of the surgery. Mice were injected with either AAV6-hSyn-ChR2 (H134R)-EYFP or AAV6-hSyn-EYFP control virus (University of Minnesota Viral Vector Core; maps are presented in Supplementary Figure 1) into the BAT. The AAV6 serotype was chosen due to its documented ability to be taken up by neuronal terminals and transported in a retrograde fashion.[23,24] Each side of the tissue was injected with 3.0 μL of virus in 3-6 injection sites in order to maximize the spread of virus throughout the tissue using an approach similar to the one developed to perform the local sympathectomy with chemical agents.[25] Injections were delivered at a rate of 0.1 μL/min and needles were allowed to sit for 5 minutes after the end of each injection to allow for viral diffusion prior to needle removal. Mice began optogenetic experiments at least six weeks following injection to allow for viral transport and sufficient levels of opsin expression in the targeted terminal regions. In the weeks between surgery and test, the AAV6-ChR2 infected mice gained 2.4 ± 0.3 grams on average, while the control AAV6-EYFP mice gained 2.4 ± 0.08 grams on average, suggesting no adverse effect of the viral injection.

2.3 | Optogenetic stimulation of BAT

A custom-made implant was used to deliver blue light onto opsin-expressing adipose tissue. The implant was made using a LED (455 nm, 0805 SMD, Chanzon) that was encased in a

thin layer of polydimethylsiloxane (PMDS) and coupled to a thermoprobe (source) to allow for temperature measurements of the BAT close (~0.1-1.0 mm) to the field of blue light illumination (irradiance ~ 10 mW/mm2). Control mice not expressing the ChR2 were also exposed to blue light pulses to confirm that changes in temperature observed were not due to nonspecific light-induced heating.

For testing, mice were anesthetized under isoflurane (4% induction, 2 to 2.5% maintenance) and placed on a heating pad (33-35°C). An incision was made on the back to expose the adipose tissue and an opening was carefully made in the mid-caudal region of the BAT to allow for probe placement underneath the organ while avoiding the damage of nerves and vasculature, with the light directed upward toward the bottom ventral surface of the tissue in order to maximize tissue penetration. The probe was secured into place, the fat pad was gently lowered on top of the LED, and the skin was secured closely around the probe exit to prevent tissue drying during the experiment. An additional thermal probe was placed in the rectum to allow for simultaneous measurement of core body temperature. Next, baseline measurements were taken once a minute until both the BAT and core temperatures were stabilized (<0.2°C change over 10 minutes). Mice were then exposed to pulsed blue-light stimulation (5 ms pulse width, 20 Hz, 1 sec on / 1 sec off) as described in the result section. Both the BAT and rectal temperatures were recorded once a minute during the blue-light stimulation and data were presented as delta °C change over baseline values.

2.4 | Tissue collection and immunohistochemical (IHC) analysis

Mice were rapidly euthanized by cervical dislocation immediately after the poststimulation period, and tissue was collected for further analysis. For BAT excision, each mouse was positioned prone facing down and an incision was made with a pair of scissors at a 30° angle on the dorsal side along the midline from the neck to the lower abdomen. The skin was lifted carefully to expose the butterfly shaped BAT allowing to hold and lift the apical portion of the depot while carefully severing with scissors along the periphery of the entire area. Any superficial white adipose atop and around the butterfly was carefully removed. Half the tissue was snap frozen and stored at −80°C while half was fixed in 4% paraformaldehyde and processed for histological analysis (see below). Furthermore, an incision was made on the throat and muscle, bone, and connective tissue around the rib/clavicle area was dissected to expose the region where the brachiocephalic artery divides into the right common carotid and subclavian arteries. The sympathetic ganglia were located behind and below the subclavian artery at this division and could be identified by its star-shaped, pearly gray onion-like appearance. Once identified, the ganglion was held in place with forceps to be dissected with abundant surrounding tissue for anatomical reference.

Dissected sympathetic ganglia were immersion fixed in 4% PFA for 24 hours, then cryoprotected in 30% sucrose for 3 days. Tissue sections harvested from virus infected mice were obtained using a Leica CM 1900 cryostat and mounted onto Superfrost Plus microscope slides; they were washed two times in phosphate buffer (PB), then sections were incubated in 1:75 (vol/vol) normal donkey serum (Jackson Immuno Research; West Grove, PA) in PB for 20 minutes at room temperature to block nonspecific sites and then incubated overnight at 4°C with a primary antibody against TH (AB1542 Chemicon Millipore, Milan, Italy; 1:300). The following day tissues were washed twice in PB for 15 minutes and then incubated with Alexa Fluor 568 nm (red) to visualize TH-positive adrenergic fibers. The tissue was finally counterstained with the nuclear dye TO-PRO3 633 nm (blue). Slides were mounted with Prolong Antifade (Invitrogen). Fluorescence was detected with a Leica TCS-SL confocal microscope (Leica Microsystems, Vienna, Austria) equipped with an Argon and He/Ne mixed gas laser. Dyes were imaged separately (1024×1024 pixels) and then merged. Images were obtained using a confocal pinhole of 1.1200 and stored as TIFF files. Brightness and contrast of the final images were adjusted using the Photoshop 6 software (Adobe Systems; Mountain View, CA, USA).

Brown Adipose tissue was immersion-fixed in modified Zamboni's fixative (4% paraformaldehyde and 0.2% picric acid in 0.1 M phosphate buffer, pH 6.9), cryoprotected in 10% sucrose, and cryostat-sectioned into 30 mm section which were mounted on gel-coated slides. Sections were preabsorbed in blocking buffer (PBS containing 0.3% Triton-X 100, 1% BSA, 1% normal donkey serum) for 30 minutes, followed by incubation overnight at 4°C with appropriate primary antibodies: chicken anti-GFP (1:1000 Abcam, ab13970, Cambridge, UK), and sheep anti-TH (1:500, Millipore AB1542). After rinsing, the sections were then incubated for 1 hour at room temperature with appropriate secondary antibodies: Cy3 conjugated donkey anti-chicken and Alexa Fluor 488 conjugated donkey anti- goat secondary antibodies (1:1000, Jackson ImmunoResearch). Images were collected using an Olympus Fluoview 1000 imaging system, processed in FIJI (projection of optical sections and file format conversion) and adjusted for brightness and contrast in Adobe Photoshop CC.

To evaluate the EYFP expression specificity exclusive from CD31, fresh snap-frozen BAT was cryosectioned into 20 μm sections, and mounted onto Superfrost Plus microscope slides. The mounted sections were fixed in 4% PFA for 15 minutes then washed three times in PBS. Nonspecific binding was blocked in 2% normal donkey serum (NDS; Jackson Labs), 0.1% Triton-X 100 in PBS for 1 hour at room temperature then incubated with

primary antibodies—sheep anti-TH (1:500, Millipore AB1542), rat anti-CD31 (Dianova, DIA-310), and rabbit anti-GFP (1:500, Invitrogen A11122) in blocking solution overnight at 4°C. The following day the sections were washed three times with PBS, then incubated with secondary antibodies—donkey anti-sheep Alexa Fluor 647 (1:500, Jackson Immuno Research), donkey anti-rabbit 488 (1:500, Jackson Immuno Research), donkey anti-rat 568 (1:500; Jackson Immuno Research) in blocking solution for 1 hour at room temperature. After three washes in PBS, the slides were coverslipped with ProLong Diamond Antifade mountant (Invitrogen). The slides were imaged with a Nikon Eclipse microscope equipped with a 60× objective N.A. = 0.95, processed, and adjusted for brightness and contrast with FIJI.

Adrenal glands harvested from the transgenic mice were fixed overnight in 4% PFA then cryoprotected in 30% sucrose before they were cut into 10 μm cryosections and mounted onto Superfrost Plus microscope slides Tissue was rehydrated with three washes in PB. The tissue was blocked for 1 hour at room temperature in 2% normal donkey serum (NDS; Jackson Labs) in PB. They were then incubated with primary antibodies—sheep anti-Tyrosine Hydroxylase (1:500, Millipore AB1542) and rabbit anti-GFP (1:500, Invitrogen A11122) in 2% NDS in PB overnight at 4°C. The following day the sections were washed three times in PB. Secondary incubation was for 1 hour at room temperature with donkey anti-sheep Alexa Fluor 647 (1:200, Jackson Immuno Research) and donkey anti- rabbit 568 (1:200, Jackson Immuno Research) in 2% NDS in 1X PB. After three additional washes in PB, the slides were coverslipped with ProLong Diamond Antifade mountant (Invitrogen). The sections were imaged with a Nikon A1R Confocal microscope, 20× objective N.A. = 0.75 (University Imaging Centers, University of Minnesota). FIJI was used to quantify colocalization of TH with EYFP.

2.5 | Tissue clearing using the X-CLARITY system

The tissue was removed from the fixative, rinsed with 1× phosphate-buffered saline (PBS) several times, and then incubated in 1× PBS at 4.0°C for 24hours. Afterward the tissue was cleared using the X-Clarity System (Annandale, VA). In summary, the tissue was immersed in the X-CLARITY polymerization initiator solution and processed according to the manufacturer's instructions. The samples were incubated for 24 hours at 4.0°C, in the hydrogel monomer with accelerator and then polymerized for 3 hours at a vacuum (kPa) of −85, and a temperature of 37.0°C. The Tissue/gel was shaken for 1 minute and rinsed in 1× PBS. Subsequently samples were processed in the electrophoretic tissue clearing (ETC) solution for 20 hours (checked after 2 hours) at a current of 1.1A, temperature of 37.0°C, and pump speed of 40 rpm. Subsequently, samples were stored in 1× PBS at 4.0°C. In preparation for taking images, the samples were placed in X-CLARITY mounting solution (R.I. 1.46) for 2-4 hours. All fluorescent images were taken using the Ti-E microscope with A1R confocal Microscope using the Nikon 10X glycerol, 0.5 N.A., 5.0 mm WD objective (Nikon Instruments Melville, NY). Images were processed in Nikon Elements v4.6 or Imaris, 9.0.1 software (Bitplane, Oxford Instruments, concord, MA).

2.6 | RT-qPCR

RNA from BAT was extracted using a PureLink RNA Mini Kit (Thermo Fisher Scientific) according to the manufacturer's protocol. Transcription into cDNA was performed using the iScript cDNA synthesis kit (Bio-Rad) according to the manufacturer's directions. Each cDNA sample was run in duplicate using the iTaq Universal SYBR Green PCR Master Mix (Bio-Rad) to a final volume of 15 μL in a CFX Connect thermal cycler and optic monitor (Bio-Rad). The expression of genes was normalized to the geometric mean of two housekeeping genes – actin and transcription factor II (TFII). Sequences of primers used were: actin (forward: 5′-GGCACCACACCTTCTACAATG-3′ reverse: 5′-GGGGTGTTGAAGGTCTCAAAC-3′), TFII (forward: 5′-TGG AGA TTT GTC CAC CAT GA-3′ reverse: 5′-GAA TTG CCA AAC TCA TCA AAA CT-3′), preUCP1 (forward: 5′-GGA TTG GCC TCT ACG ACT CA-3′ reverse: 5′-GGC CAG TTG GTT TTC ACA GA-3′), and UCP1 (forward 5′-GTC CCC TGC CAT TTA CTG TCA G-3′ reverse 5′-TTT ATT CGT GGT CTC CCA GCA TAG). Data was analyzed using the $\Delta\Delta C_t$ method.

2.7 | Statistical analysis

All statistics were performed with Statistica software (Tibco). Data were expressed as mean +/− SEM unless otherwise specified. We first compared the response of males and females and, after excluding a significant sex effect, data were pooled according to the experimental treatment. Data were analyzed using repeated measures or one-way ANOVAs followed when significant by Fisher LSD post hoc tests for binary comparisons. The area under the curve was calculated using the trapezoid method. Differences were considered significant at $P < .05$.

3 | RESULTS

We engineered AAV6 to express the blue light-sensitive cation channel ChR2 fused to enhanced yellow fluorescent protein (EYFP), under the control of the pan-neuronal human

synapsin-1 promoter (hSyn).[26] We injected retrograde hSyn-AAV6-ChR2-EYFP or hSyn-AAV6-EYFP control viruses in the BAT of C57BL/6J WT mice. Immunohistochemical analysis confirmed that AAV6-transfected TH-positive sympathetic nerves[23,27,28] and not adipocytes[29] in the BAT and sympathetic ganglia (Supplementary Figure 2A-I). In particular, colocalization of EYFP and TH staining was detected in correspondence of neuronal bodies within ganglia, and nerve fibers in the BAT (Supplementary Figure 2J-M).

Six weeks after the surgery, mice injected with AAV6-ChR2-EYFP or AAV6-EYFP or uninfected controls were anesthetized and stimulated with blue LED light with the BAT and core temperatures being simultaneously recorded (Figure 1A). The LED and thermal probe were positioned under the BAT taking care not to damage the nerves or the vasculature. Using a 30min light ON protocol we showed rapid and consistent rise in the BAT and core temperatures in ChR2 expressing mice but not in AAV6-EYFP or uninfected control mice (Figure 1B,C,E,F), as highlighted by a statistically significant main effect of the virus during the stimulation time-course (BAT: $F(2,13) = 6.98$, $P < .003$; Rectal: $F(2,13) = 8.46$, $P < .005$) as well as of the area under the curve (BAT: $F(2,13) = 6.48$, $P < .05$; Rectal: $F(2,13) = 7.92$, $P < .006$). This stimulation protocol was also effective in inducing a significant increase in transcriptional activation of UCP1 (measuring of the nascent preUCP1 transcript[30,31]) in ChR2 expressing mice when compared to controls (Figure 1D). The optogenetic–induced thermogenic effect was confirmed in a second ON-OFF protocol with the duration of the rise in temperature corresponding to the duration of the tissue illumination (Supplementary Figure 3A). To further corroborate this result we engineered the same construct described above using a second virus expressing tdTomato that led to a comparable rise of BAT temperature upon optogenetic stimulation (Supplementary Figure 3B).

Overall, these data demonstrate that our viral construct can efficiently transfect sympathetic neurons in the BAT and that optogenetic neuromodulation of ChR2 expressing nerves

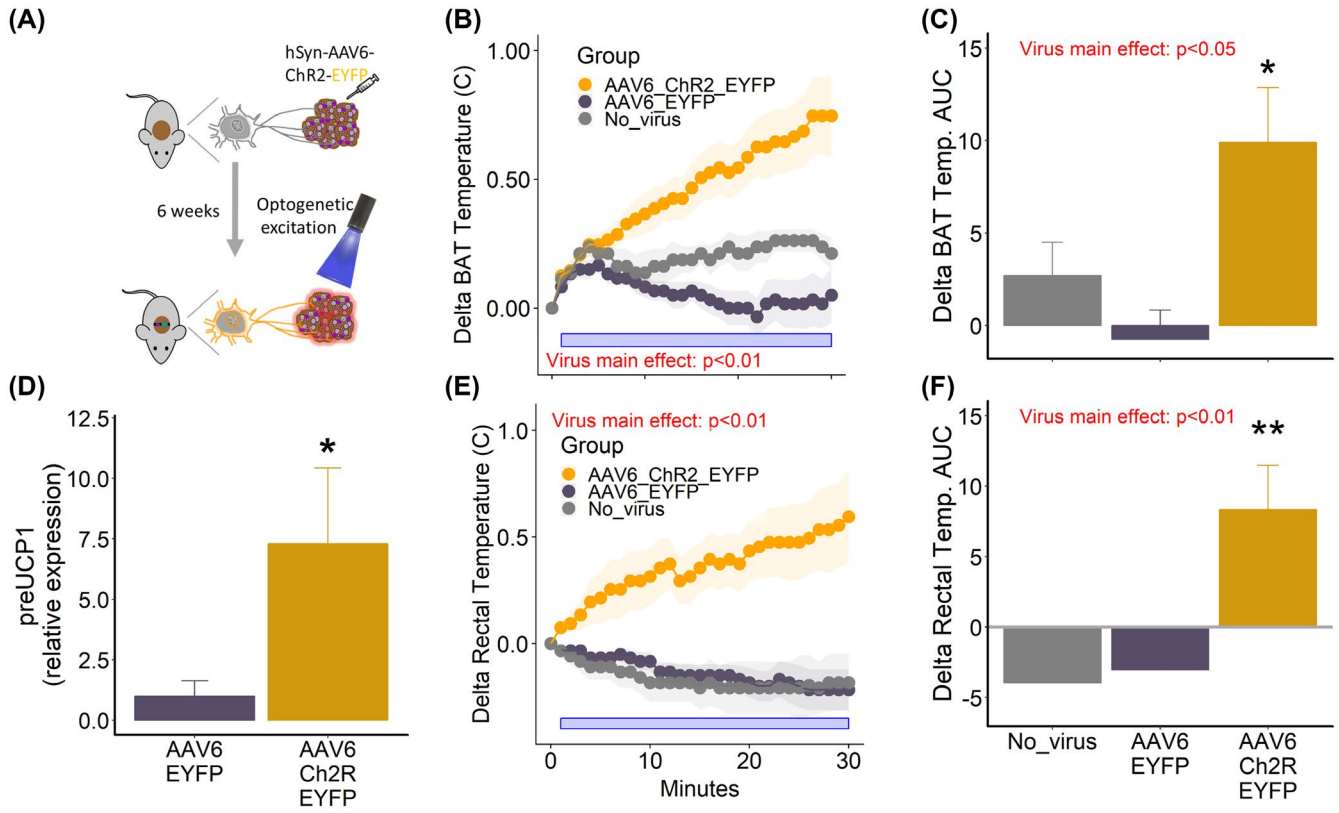

FIGURE 1 Brown Adipose Tissue (BAT) optogenetic stimulation in channelrhodopsin (ChR2) virally-infected mice elicits thermogenesis. (A) Illustration of the experimental procedure. BAT (B) and rectal (E) temperature change vs unstimulated preparation during 30 minutes (unstimulated average BAT temperatures +/− SEM: AAV6_ChR2_EYFP: 32.32 +/− 0.34°C; AAV6_EYFP: 32.8 +/− 0.30°C; No_virus: 30.81 +/− 0.69°C; unstimulated average core temperatures +/- SEM: AAV6_ChR2_EYFP: 34.24 +/− 0.81°C; AAV6_EYFP: 35.1 +/− 0.28°C; No_virus: 34.18 +/−0.47°C). Cumulative BAT (C) and rectal (F) temperature change vs unstimulated preparation expressed as Area Under the Curve (AUC) during 30 min stimulation under anesthesia. D) The preUCP1 RNA expression level from BAT was collected at the end of the recording. AAV6-ChR2-EYFP, channelrhodopsin infected mice; AAV6- EYFP, virus control mice, No virus, uninfected mice. (N = 5-7). The horizontal blue bar represents the duration of the LED stimulation. Data represent group averages +/− SEM. *indicates $P < .05$; **indicates $P < .01$

is sufficient to elicit BAT activation. Importantly our two control groups exclude a role for the virus and the LED stimulation per se on BAT thermogenesis.

Next, we aimed to validate our viral-mediated approach by using a genetic mode, TH-Cre X Rosa26-LSL-ChR2-YFP mice as previously established[22] (referred to as ChR2$^{TH\text{-}Cre+}$ or ChR2$^{TH\text{-}Cre-}$) (Figure 2A). ChR2$^{TH\text{-}Cre+}$ mice express Cre-recombinase under a TH promoter in catecholaminergic neurons thus driving the selective expression of the blue light-sensitive ChR2 and EYFP in the sympathetic fibers innervating the BAT (Supplementary Figure 4). Colocalization of TH and EYFP in the chromaffin cells in the adrenal gland for positive control was confirmed using IHC (Supplementary Figure 5). EYFP fluorescence was also confirmed using X-Clarity (Supplementary Figure 6 and Supplementary Video 1). Furthermore, EYFP does not colocalize with the endothelial marker CD31 and there was no EYFP expression in TH negative regions (Supplementary Figure 4), thus confirming the specificity of TH-driven expression, in the present experimental condition. Next, ChR2$^{TH\text{-}Cre+}$ or ChR2$^{TH\text{-}Cre-}$ mice were tested in our acute optogenetic preparation with 30 minutes LED ON:OFF. Consistent with the data obtained with AAV6-ChR2 infected mice, optogenetic stimulation of the sympathetic nerves elicited BAT, and Core thermogenesis in ChR2$^{TH\text{-}Cre+}$ but not in ChR2$^{TH\text{-}Cre-}$ mice (Figure 2). Specifically, 30 minutes optogenetic stimulation gradually and significantly elevated both the BAT and rectal temperatures in ChR2$^{TH\text{-}Cre+}$ mice, as indicated by the shape of the trajectory of the increase (BAT: $F(1,9) = 11.95$, $P < .008$; core: $F(1,9) = 5.98$, $P < .05$) (Figure 2C,D), as well as by the cumulative degree of increase for the whole 30 minutes stimulation (BAT: $F(1,9) = 11.82$, $P < .008$; core $F(1,9) = 6.18$, $P < .05$) (Figure 2E-H). After the LED was turned OFF, the BAT temperature trended to decrease while, as expected,[32] the core temperature continued to rise (Figure 2A,D). Finally, optogenetic excitation of the sympathetic nerves corresponded to a significant increase of the expression of preUCP1 RNA in ChR2$^{TH\text{-}Cre+}$ when compared to ChR2$^{TH\text{-}Cre-}$ mice ($P < .05$) (Figure 2B). Consistent with previous data in cold-exposed mice,[31,33] 30 minutes optogenetic nerve stimulation was not sufficient to increase the expression of mature UCP1 mRNA (ChR2$^{TH\text{-}Cre}$ = 1 ± 0.28, ChR2$^{TH\text{-}Cre+}$ = 0.54 ± 0.12, NS). The 30 minutes optogenetic-induced increase in the BAT and core temperatures was larger in ChR2$^{TH\text{-}Cre+}$ when compared to the AAV6-ChR2 mice from the previous experiment (Supplementary Figure

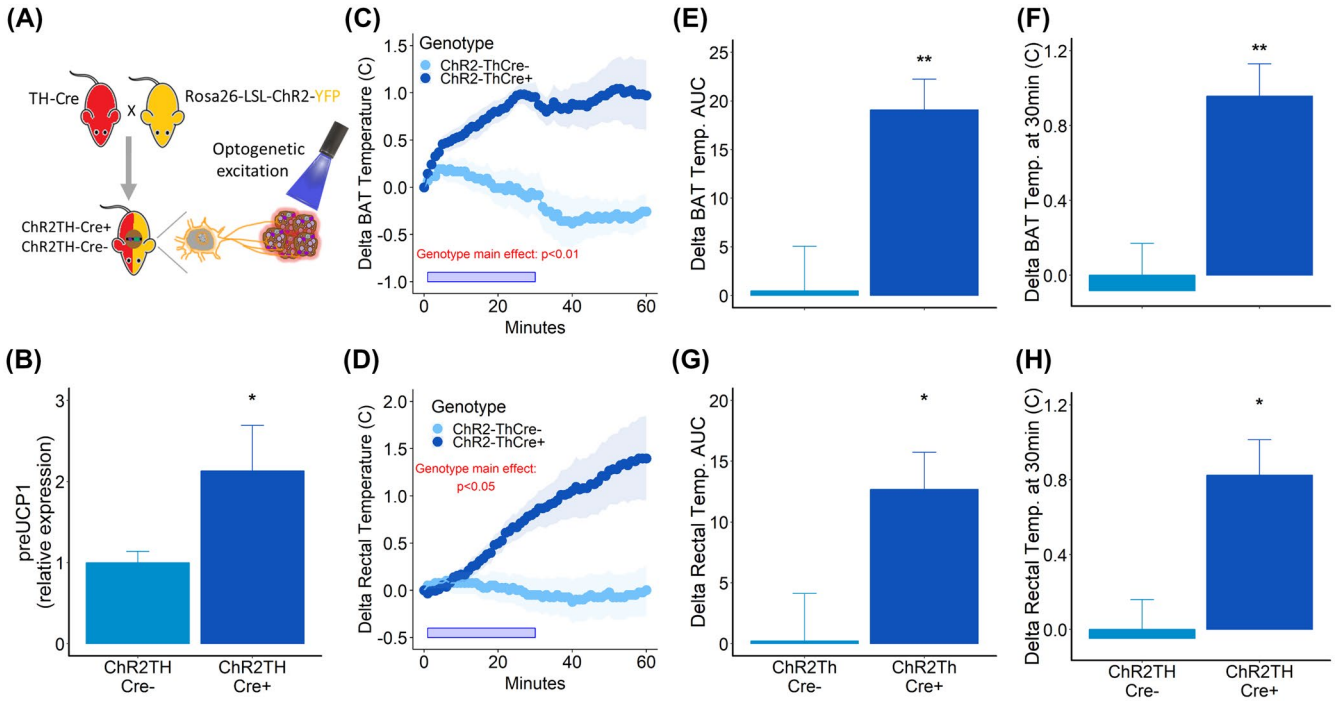

FIGURE 2 Brown Adipose Tissue (BAT) optogenetic stimulation in mice genetically expressing channelrhodopsin (ChR2) in sympathetic nerves elicits thermogenesis. (A) Illustration of the experimental procedure. (B) Optogenetic excitation increased preUCP1 RNA in ChR2$^{TH\text{-}Cre+}$ mice. N = 5-7, half male half females per group. (C) BAT and (D) rectal temperature change vs unstimulated preparation during 30 minutes stimulation and 30 minutes following the end of stimulation (unstimulated average BAT temperatures +/− SEM: ChR2-ThCre-: 30.9 +/− 0.86°C; ChR2-ThCre+: 31.4 +/− 0.53°C; unstimulated average core temperatures +/− SEM: ChR2-ThCre-: 33.6 +/− 0.49°C; ChR2-ThCre+: 33.6 +/− 0.52°C). Cumulative BAT (E) and rectal (G) temperature change vs unstimulated preparation expressed as AUC during 30 min stimulation under anesthesia. BAT (F) and Rectal (H) temperature change vs unstimulated preparation at the end of the stimulation phase. (N = 4-7). The horizontal blue bar in C and D represents the duration of the LED stimulation. Data represent group averages +/− SEM. *indicates $P < .05$, **indicates $P < .01$

3C,D). Overall, our second strategy, where the expression of the genetic construct was driven in sympathetic neurons through breeding targeted genetic mouse lines, confirmed that optogenetic excitation of ChR2-expressing neurons is sufficient for BAT thermogenesis, where none was elicited in noncarrier control mice.

4 | DISCUSSION

Using two independent approaches, we demonstrated that optogenetic neuromodulation is sufficient to elicit BAT and core thermogenesis and stimulate the expression of pre-UCP1 RNA in BAT. More broadly, this research contributes to the field of optogenetic manipulation of the peripheral nervous system (PNS), which as a whole is far less developed than that of the central nervous system (CNS).[21,22,34]

For opsin virus mediated transfection, we used AAV6, which has been used for gene delivery through retrograde transport both in the periphery[35] and in the brain,[24] and is of translational relevance since AAV vectors belong to the first gene therapy products approved by FDA and are currently tested in the clinical trials for human diseases.[36,37] We engineered AAV6 to express the ChR2 fused to the fluorescent reporter EYFP, under the control of hSyn to restrict the transgene expression from an adenoviral vector exclusively to neurons.[38] In our hands, this strategy was successful as demonstrated by the specific staining of sympathetic neurons, both in cell bodies and in fibers proximal to the brown adipocytes.[22,39,40] Furthermore, we functionally characterized the thermogenic response evoked in ChR2 infected mice by optogenetic stimulation both at the BAT and the systemic level. This result is further evidenced by the significant induction of the preUCP1 RNA (the nascent UCP1 transcript[30,31]) in ChR2 infected mice compared to controls. One limitation of our present study is that experiments were conducted under general anesthesia, which is known to cause hypothermia.[41] This choice of gas anesthesia was consistent with previous protocols[21,42] as well as the need to have a physiologically stable experimental preparation over an extended period of time, without the need for periodic re-dosing as required with chemical anesthetics.

It must be noted that the application of optogenetic stimulation of nerves outside the CNS has been limited due to intrinsic properties of the PNS. The Opsin expression in the PNS can be reduced by immune responses induced by viral vector injection, a consequence of the higher degree of immune surveillance in the PNS compared to that of the CNS.[26,43] Furthermore, the distribution of excitable cells is sparsely scattered throughout the target tissue, necessitating broader reach of illumination, which can also be impaired by the opaqueness of the target tissue.[34] To overcome these limitations and to aim at a more efficient optogenetic stimulation of the BAT, we adapted a previously validated approach to generate a genetic mouse model expressing the opsin under the control of a TH-Cre promoter that limited the opsin expression to the sympathetic fibers innervating the BAT adapting.[21,22] Many Cre-driver lines are still not fully characterized in the PNS. Thus, one additional value of the characterization we conducted of our $ChR2^{TH\text{-}Cre+}$ model is to elucidate the features of the opsin expression in the sympathetic nerves innervating peripheral organs, but not CD31 positive cells, expanding on what already demonstrated for other adipose depots.[21,22] For example, a combination of intravital two-photon microscopy and local optogenetic stimulation of sympathetic inputs illustrated on how sympathetic nerve fibers establish neuro-adipose junctions, directly encasing adipocytes, and locally induce lipolysis and loss of white adipose mass.[22] Previous data showed that optogenetically induced thermogenesis was dependent on intracellular glycolysis, identifying glucose as a critical substrate that fuels acute BAT function.[21] In-line with these results, the optogenetic stimulation of the sympathetic nerves led to appreciably rapid temperature rises both at the BAT and at the systemic level in $Ch2R^{TH\text{-}Cre+}$ and AAV6-ChR2 infected mice while it failed to do so in $Ch2R^{TH\text{-}Cre-}$ or the two controls groups used for the virus study. Consistent with sympathetic-mediated brown adipocyte activation in both virally injected and genetically induced models, optogenetic excitation of the sympathetic nerves increased the expression of preUCP1 RNA in ChR2-expressing mice when compared to controls.

5 | CONCLUSION

In conclusion, our experimental approach validated the use of retrograde viral transfection and of genetically driven expression of genetic constructs to sympathetic nerves innervating BAT. We also demonstrated that the targeted and selective optogenetic activation of the sympathetic nerves expressing the opsin is sufficient to elicit selective BAT and core thermogenesis, as well as transcriptional regulation of UCP1. Our results add to the existing literature supporting the notion that peripheral neuromodulation could be therapeutically exploited to manipulate the BAT potent catabolic function as an alternative therapeutic option for the treatment of obesity and obesity-associated diseases.

ACKNOWLEDGMENTS

Supported by Wallin Neuroscience Discovery Fund, DK117504, DK102496, DK118150, and DK102496-02S1 to AB and RSA-Frontini (UNIVPM) to AF. We would like to thank the MnDRIVE Optogenetics Core and for technical support for the optogenetic experiment, the Viral Vector and Cloning Core for designing and packaging the AAV,

the University Imaging Centers, http://uic.umn.edu for the X-Clarity and support with IHC experiments. Madeline Berg is acknowledged for technical assistance.

CONFLICT OF INTEREST

None declared.

AUTHOR CONTRIBUTIONS

C.E. Lyons, M. Razzoli, E. Larson, D. Svedberg, A. Frontini, L. Vulchanova, M. Sanders, performed experiments and analyzed data; S. Cinti, M. Thomas, and M. Sanders contributed reagents and helped conceptualize the research; A. Bartolomucci conceptualized the research and obtained funding. C.E. Lyons, M. Razzoli, and A. Bartolomucci wrote the manuscript with input from all co-authors.

REFERENCES

1. Cannon B, Nedergaard J. Brown adipose tissue: function and physiological significance. *Physiol Rev*. 2004;84:277-359.
2. Peirce V, Vidal-Puig A. Regulation of glucose homoeostasis by brown adipose tissue. *Lancet Diabetes Endocrinol*. 2013;1:353-360.
3. Bartelt A, Bruns OT, Reimer R, et al. Brown adipose tissue activity controls triglyceride clearance. *Nat Med*. 2011;17:200-205.
4. Cypess AM, Lehman S, Williams G, et al. Identification and importance of brown adipose tissue in adult humans. *N Engl J Med*. 2009;360:1509-1517.
5. Cypess AM, Weiner LS, Roberts-Toler C, et al. Activation of human brown adipose tissue by a β3-adrenergic receptor agonist. *Cell Metab*. 2015;21:33-38.
6. Leitner BP, Huang S, Brychta RJ, et al. Mapping of human brown adipose tissue in lean and obese young men. *Proc Natl Acad Sci USA*. 2017;114:8649-8654.
7. Xue R, Lynes MD, Dreyfuss JM, et al. Clonal analyses and gene profiling identify genetic biomarkers of the thermogenic potential of human brown and white preadipocytes. *Nat Med*. 2015;21:760-768.
8. Shinoda K, Luijten IHN, Hasegawa Y, et al. Genetic and functional characterization of clonally derived adult human brown adipocytes. *Nat Med*. 2015;21:389-394.
9. Morrison SF, Madden CJ, Tupone D. Central neural regulation of brown adipose tissue thermogenesis and energy expenditure. *Cell Metab*. 2014;19:741-756.
10. Kataoka N, Hioki H, Kaneko T, Nakamura K. Psychological stress activates a dorsomedial hypothalamus-medullary raphe circuit driving brown adipose tissue thermogenesis and hyperthermia. *Cell Metab*. 2014;20:346-358.
11. Razzoli M, Frontini A, Gurney A, et al. Stress-induced activation of brown adipose tissue prevents obesity in conditions of low adaptive thermogenesis. *Mol Metab*. 2016;5:19-33.
12. Razzoli M, Bartolomucci A. The dichotomous effect of chronic stress on obesity. *Trends Endocrinol Metab*. 2016;27:504-515.
13. Bachman SE, Dhillon H, Zhang CY, et al. βAR signaling required for diet-induced thermogenesis and obesity resistance. *Science (80-.)*. 2002;297:843-845.
14. Xiao C, Goldgof M, Gavrilova O, Reitman ML. Anti-obesity and metabolic efficacy of the β3-adrenergic agonist, CL316243, in mice at thermoneutrality compared to 22°C. *Obesity (Silver Spring)*. 2015;23:1450-1459.
15. Rondini EA, Mladenovic-Lucas L, Roush WR, Halvorsen GT, Green AE, Granneman JG. Novel pharmacological probes reveal ABHD5 as a locus of lipolysis control in white and brown adipocytes. *J Pharmacol Exp Ther*. 2017;363:367-376.
16. Lee YH, Petkova AP, Konkar AA, Granneman JG. Cellular origins of cold-induced brown adipocytes in adult mice. *FASEB J*. 2015;29:286-299.
17. Betz MJ, Enerbäck S. Human brown adipose tissue: what we have learned so far. *Diabetes*. 2015;64:2352-2360.
18. Kajimura S, Saito M. A new era in brown adipose tissue biology: molecular control of brown fat development and energy homeostasis. *Annu Rev Physiol*. 2014;76:225-249.
19. Saito M, Okamatsu-Ogura Y, Matsushita M, et al. High incidence of metabolically active brown adipose tissue in healthy adult humans: effects of cold exposure and adiposity. *Diabetes*. 2009;58:1526-1531.
20. Bartolomucci A, La Corte G, Possenti R, et al. TLQP-21, a VGF-derived peptide, increases energy expenditure and prevents the early phase of diet-induced obesity. *Proc Natl Acad Sci U S A*. 2006;103(39):14584–9.
21. Jeong JH, Chang JS, Jo Y-H. Intracellular glycolysis in brown adipose tissue is essential for optogenetically induced nonshivering thermogenesis in mice. *Sci Rep*. 2018;8:6672.
22. Zeng W, Pirzgalska RM, Pereira MMA, et al. Sympathetic neuro-adipose connections mediate leptin-driven lipolysis. *Cell*. 2015;163:84-94.
23. Salegio EA, Samaranch L, Kells AP, et al. Axonal transport of adeno-associated viral vectors is serotype-dependent. *Gene Ther*. 2013;20:348-352.
24. San Sebastian W, Samaranch L, Heller G, et al. Adeno-associated virus type 6 is retrogradely transported in the non-human primate brain. *Gene Ther*. 2013;20:1178-1183.
25. Rooks CR, Penn DM, Kelso E, Bowers RR, Bartness TJ, Harris RBS. Sympathetic denervation does not prevent a reduction in fat pad size of rats or mice treated with peripherally administered leptin. *Am J Physiol Integr Comp Physiol*. 2005;289:R92-R102.
26. Iyer SM, Montgomery KL, Towne C, et al. Virally mediated optogenetic excitation and inhibition of pain in freely moving nontransgenic mice. *Nat Biotechnol*. 2014;32:274-278.
27. Madisen L, Mao T, Koch H, et al. A toolbox of Cre-dependent optogenetic transgenic mice for light-induced activation and silencing. *Nat Neurosci*. 2012;15:793-802.
28. Towne C, Pertin M, Beggah AT, Aebischer P, Decosterd I. Recombinant adeno-associated virus serotype 6 (rAAV2/6)-mediated gene transfer to nociceptive neurons through different routes of delivery. *Mol Pain*. 2009;5:52. doi: https://doi.org/10.1186/1744-8069-5-52.
29. Uhrig-Schmidt S, Geiger M, Luippold G, et al. Gene delivery to adipose tissue using transcriptionally targeted rAAV8 vectors. *PLoS ONE*. 2014;9:e116288.
30. Razzoli M, Emmett MJ, Lazar MA, Bartolomucci A. β-Adrenergic receptors control brown adipose UCP-1 tone and cold response without affecting its circadian rhythmicity. *FASEB J*. 2018;32:5640-5646.
31. Gerhart-Hines Z, Feng D, Emmett MJ, et al. The nuclear receptor Rev-erbα controls circadian thermogenic plasticity. *Nature*. 2013;503:410-413.
32. Morrison SF. Efferent neural pathways for the control of brown adipose tissue thermogenesis and shivering. *Handb Clin Neurol*. 2018;156:281-303.

33. Chappuis S, Ripperger JA, Schnell A, et al. Role of the circadian clock gene Per2 in adaptation to cold temperature. *Mol Metab*. 2013;2:184-193.
34. Montgomery KL, Iyer SM, Christensen AJ, Deisseroth K, Delp SL. Beyond the brain: optogenetic control in the spinal cord and peripheral nervous system. *Sci Transl Med*. 2016;8:337rv5.
35. Towne C, Montgomery KL, Iyer SM, Deisseroth K, Delp SL. Optogenetic control of targeted peripheral axons in freely moving animals. *PLoS ONE*. 2013;8:e72691.
36. Asokan A, Schaffer DV, Jude Samulski R. The AAV vector toolkit: poised at the clinical crossroads. *Mol Ther*. 2012;20:699-708.
37. Dunbar CE, High KA, Joung JK, Kohn DB, Ozawa K, Sadelain M. Gene therapy comes of age. *Science*. 2018;359:175.
38. Kügler S, Kilic E, Bähr M. Human synapsin 1 gene promoter confers highly neuron-specific long-term transgene expression from an adenoviral vector in the adult rat brain depending on the transduced area. *Gene Ther*. 2003;10:337-347.
39. Giordano A, Morroni M, Santone G, Marchesi GF, Cinti S. Tyrosine hydroxylase, neuropeptide Y, substance P, calcitonin gene-related peptide and vasoactive intestinal peptide in nerves of rat periovarian adipose tissue: an immunohistochemical and ultrastructural investigation. *J Neurocytol*. 1996;25:125-136.
40. Giordano A, Frontini A, Cinti S. Adipose organ nerves revealed by immunohistochemistry#. In: Yang K. (eds) *Adipose Tissue Protocols. Methods in Molecular Biology*™, vol 456. Humana Press. 2008:83-95.
41. Swindle MM, Vogler GA, Fulton LK, Marini RP, Popilskis S. Preanesthesia, anesthesia, analgesia, and euthanasia. *Lab Anim Med*. 2002;955-1003.
42. Bell BB, Harlan SM, Morgan DA, Guo D-F, Cui H, Rahmouni K. Differential contribution of POMC and AgRP neurons to the regulation of regional autonomic nerve activity by leptin. *Mol Metab*. 2018;8:1-12.
43. Sack BK, Herzog RW. Evading the immune response upon in vivo gene therapy with viral vectors. *Curr Opin Mol Ther*. 2009;11:493-503.

SUPPORTING INFORMATION

Additional supporting information may be found online in the Supporting Information section.

How to cite this article: Lyons CE, Razzoli M, Larson E, et al. Optogenetic-induced sympathetic neuromodulation of brown adipose tissue thermogenesis. *The FASEB Journal*. 2019;00:1–9. https://doi.org/10.1096/fj.201901361RR